

# Integrated microfluidic viscometer equipped with fluid temperature controller for measurement of viscosity in complex fluids

Yang Jun Kang · Sung Yang

Received: 2 July 2012 / Accepted: 13 October 2012 / Published online: 22 November 2012  
© Springer-Verlag Berlin Heidelberg 2012

**Abstract** In the study described herein, a microfluidic viscometer equipped with fluid temperature controller is proposed for measuring the viscosity of complex liquids containing cells or particles. The microfluidic viscometer is composed of a microfluidic device and a fluid temperature controller. The microfluidic device has two inlets, for the introduction of the sample and reference fluids, respectively, and a spacious diverging channel with a large number of identical indicating channels. A fluid temperature controller, which contained a Peltier chip, micro thermocouples, and a feedback controller, is applied for the consistent control of the temperature of the fluids in the microfluidic channels. For accurately identifying fluid viscosity, an effective design criterion is discussed using an enhanced mathematical model for complex fluid networks. The accuracy of the proposed model is sufficiently investigated via numerical simulations as well as experimental measurements. As performance demonstrations, pure

liquids [five different concentrations of SDS (Sodium Dodecyl Sulphate)] and complex fluids (four different blood samples) were used to evaluate the performance of the proposed microfluidic viscometer. This investigation indicated that the proposed microfluidic viscometer is capable of accurately and simply measuring both Newtonian and non-Newtonian fluids, even without the need for calibration procedures, and artifacts faced with a conventional viscometer. We therefore conclude that our proposed microfluidic viscometer has considerable potential for the precise and easy measurement of complex fluid viscosity.

**Keywords** Microfluidic viscometer · Blood viscosity · Complex fluid viscosity · Fluid temperature controller · Microfluidic channel array

## 1 Introduction

A fluid viscometer is one of the most important analytical tools available for the accurate investigation of the rheological properties of a fluid. There is therefore a high demand for these instruments in the fields of chemistry, biology, and biomedical engineering, especially those that are rapid and accurate.

Two types of viscometer are available commercially: a cone and plate viscometer and a capillary viscometer. In the first case, the sample fluid is subject to a shear between a rotating cone and a stationary plate. The fluid viscosity is determined by measuring the torque that must be applied to turn the cone at a particular angular velocity. This viscometer is therefore able to analyse various rheological behaviours for both Newtonian and non-Newtonian fluids. However, it suffers from a number of drawbacks, in that it is expensive. It requires a large sample (~1 mL), and the

---

**Electronic supplementary material** The online version of this article (doi:10.1007/s10404-012-1085-5) contains supplementary material, which is available to authorized users.

---

Y. J. Kang · S. Yang (✉)

School of Mechatronics, Gwangju Institute of Science and Technology (GIST), 123 Cheomdan-gwagiro (Oryong-dong), Buk-gu, Gwangju, Republic of Korea  
e-mail: syang@gist.ac.kr

S. Yang

Department of Nanobio Materials and Electronics, Gwangju Institute of Science and Technology (GIST), Gwangju, Republic of Korea

S. Yang

Department of Medical System Engineering, Gwangju Institute of Science and Technology (GIST), Gwangju, Republic of Korea

test is time-consuming ( $\sim 1$  h per sample). Furthermore, this method involves lengthy washing processes, requires repeated tests to be carried out for reliability, and is only available to expert users. In a capillary viscometer, a test fluid is forced to flow through a capillary tube. The viscosity of the fluid is determined from measurements that use a pressure sensor and a flow meter. Unlike the cone and plate viscometer, the capillary viscometer is relatively inexpensive, simple to use, and mostly limited to Newtonian fluids. In order to overcome the limitations of these conventional viscometers, several research groups have recently suggested methods for the measurement of fluid viscosity that use a microfluidic platform.

Compared to the conventional viscometers described above, a microfluidic viscometer has several advantages including its relatively low cost, small volume consumption, short measurement time (1 min or less), and easy handling. Perhaps most significantly, a microfluidic viscometer does not use a washing process, and is able to measure accurately the viscosity of pure liquids. Several approaches have been used to measure the viscosity of fluids with a microfluidic platform, including both sensor-based (Chevalier and Ayala 2008) and sensorless-based (Guillot et al. 2006; Lan et al. 2010) methods, a capillary-based method (Han et al. 2007; Srivastava et al. 2005), optical tweezing (Keen et al. 2009), electrowetting (Lin et al. 2007), and resonant frequency (Quist et al. 2006). Among these, the sensor-based and the sensorless methods are capable of measuring the viscosity of a fluid in hydrodynamically continuous fluidic flows via either a syringe pump or a pressure tank. A discussion of the technical issues associated with two methods now follows.

In order to determine the viscosity of a fluid using the sensor-based method, the test fluid is delivered into a microchannel at known flow rates. The resulting changes in pressure are then measured by external bulk pressure sensors (Kang et al. 2005) or integrated pressure sensors (Pipe et al. 2008). As the pressure drop measured by the external pressure sensors includes an inevitable pressure drop in the connecting tubes as well as one in the microfluidic channel, the pressure drop in the connecting tubes should be compensated in the viscosity measurement for each fluid (Guillot et al. 2006). In addition, the integrated pressure sensor is composed of complex multilayer structures that require a relatively complex process of microfabrication. This method might not provide reliable results for low viscosity fluid due to the low threshold of the pressure sensors that result from the high flexibility of silicon-based membranes. Finally, due to the inherent nonlinear behaviours (output vs. pressure), this sensor-based method also requires the use of complex sets of calibrations with a standard sample fluid.

Compared with the sensor-based method, the sensorless-based method (Guillot et al. 2006; Lee and Tripathi 2005;

Nguyen et al. 2008) is used to measure the viscosity of a fluid by measuring a parallel flow, rather than by means of a pressure sensor, at known flow rates. This method is relatively easy to use owing to its simple setup and the absence of direct measurements of pressure. In the sensorless-based method, the relative viscosity of a sample fluid in relation to a reference fluid can be determined by the detection of the interfacial curvature between the two fluids in a single microchannel. However, this method requires image processing using a complex mathematical formula in order to determine the fluid viscosity accurately at a known shear rate (Nguyen et al. 2008). In addition, this method is still difficult to calculate the interfacial curvature with sufficient accuracy because the interfacial curvature is unexpectedly changed depending on relative viscosity and flow rate conditions, which leads to difficult problems in estimating wall shear rates for non-Newtonian fluids. For this reason, the sensorless-based method might not perform well for complex fluids that contain cells or particles. Furthermore, at low shear rates, the sensorless-based method suffers from relatively large measurement errors because the interfacial curvature is not clear (Guillot et al. 2006). In view of these drawbacks, the sensorless-based method would be appropriate for pure liquids without particulates or cells, and primarily at high shear rates (Guillot et al. 2008; Lan et al. 2010).

Recently, we have proposed a fluid viscosity identification method which makes use of a microfluidic channel array (MCA) with indicating channels (Kang et al. 2010). This proposed methodology has been demonstrated using a simple mathematical model that only focuses on indicating channels. However, the mathematical model did not sufficiently account for complex fluidic networks, and appropriately provided design criteria for effective fluid viscosity measurement. In addition, the proposed method was still required to be evaluated through numerical simulations as well as experimental measurements comprehensively.

Thus, in this study, we discuss an effective design criterion for accurate fluid viscosity measurement in details. In addition, an enhanced viscosity formula is analytically derived using a lumped parameter modeling technique for a complex microfluidic network. Furthermore, the accuracy of the viscosity formula has been extensively evaluated through numerical simulations as well as experimental measurements. Through the consideration of the temperature dependency of the viscosity of the fluid, the temperature of the fluid within the microfluidic channel is maintained with precision by means of a fluid temperature controller (which consists of a Peltier chip, micro thermocouples, and a feedback controller). In order to investigate the performance of the proposed microfluidic viscometer in detail, we measured the viscosity of Newtonian fluids

[five different concentrations of SDS (Sodium Dodecyl Sulphate)], as well as of non-Newtonian fluids (four different blood samples).

## 2 Integrated microfluidic viscometer

### 2.1 Design criterion for accurate measurement of fluid viscosity

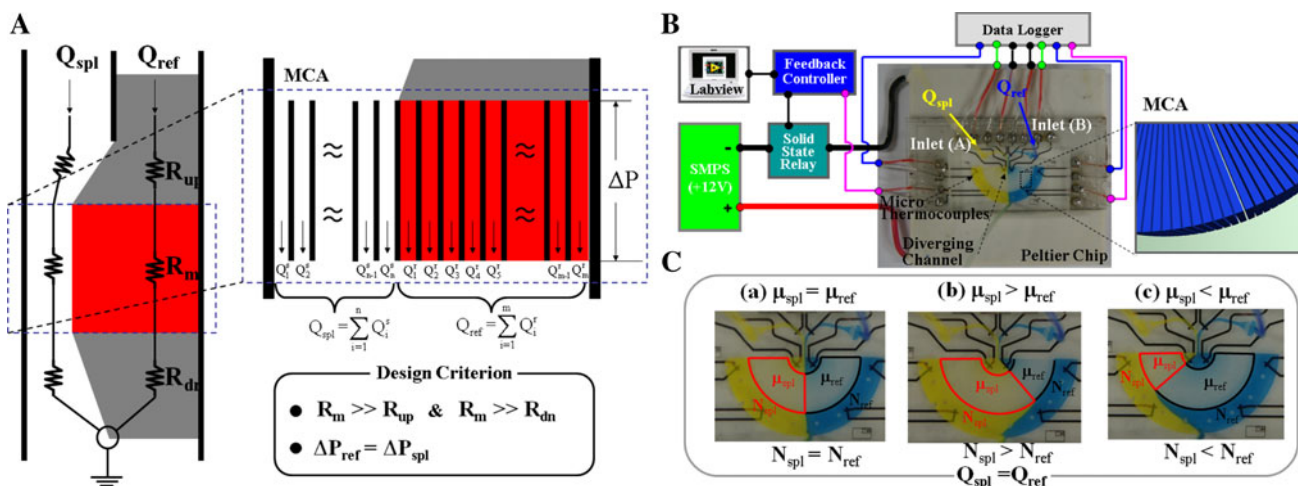
In this study described herein, the fluid viscosity measurement method would identify accurately and easily the relative viscosity ( $\mu_r = \mu_{spl}/\mu_{ref}$ ) of a sample fluid in relation to that of a reference fluid, simply by counting the number of indicating channels that become filled with each fluid within the MCA for a set of given flow rates ( $Q_{spl}, Q_{ref}$ ).

Figure 1A illustrates the viscosity measurement method, which utilizes the MCA with several identical indicating channels under parallel flows. To demonstrate the fluid viscosity measurement method, the conceptual device is divided into three sections: an upstream channel, several numbers of indicating channels with identical dimensions, and a downstream channel. The sample and reference fluids are co-infused into the upstream channel at the flow rates  $Q_{ref}$  and  $Q_{spl}$ , respectively. In here, the reference fluid is selected as a Newtonian fluid with a known viscosity that is independent of the shear rates. In order to determine the viscosity of the sample fluid within the MCA, the fluidic resistance ( $R_m$ ) of the MCA is designed to be much greater than the fluidic resistance ( $R_{up}$ ) of the upstream channel (i.e.,  $R_m \gg R_{up}$ ), and that ( $R_{dn}$ ) of the downstream channel

(i.e.,  $R_m \gg R_{dn}$ ). The global fluidic resistance is therefore dominated by the fluidic resistance of the MCA. In addition, the pressure drop for each indicating channel is identical for each fluid. To satisfy this same pressure drop ( $\Delta P_{ref} = \Delta P_{spl}$ ), the number of indicating channels filled with sample and reference fluids are precisely determined, and depends on the viscosity of the sample fluid in relative to the reference fluid for the given flow rate. Thus, the viscosity of the sample fluid relative to the reference fluid is precisely and easily identified by counting the number of indicating channels that become filled with each fluid, particularly when the flow rates are the same (i.e.,  $Q_{spl} = Q_{ref}$ ).

### 2.2 Prototype of an integrated microfluidic viscometer

In order to investigate the fluid viscosity measurement method, we developed a prototype of a microfluidic viscometer equipped with a fluid temperature controller, as shown in Fig. 1B. This microfluidic viscometer was composed of two parts. The first part was a microfluidic device, which was integrated with eight micro thermocouples, and which delivered the sample and reference fluids, monitored the temperature of the fluid, and measured the relative viscosity of the sample fluid in relation to the reference fluid. The second part was a Peltier chip, which was equipped with a feedback controller, which controlled the temperature of the fluids in the microfluidic device (see Electronic Supplementary Material-Fig. S1). The microfluidic device was designed to have (a) two inlets, for the introduction of the sample and reference fluids; (b) a diverging channel with a spacious arc shape designed to



**Fig. 1** A Schematic illustration of a prototype of the proposed microfluidic viscometer equipped with fluid temperature controller. A Fluid viscosity measurement method via a microfluidic channel array (MCA) with identical indicating channels under parallel flows. B The prototype of the microfluidic viscometer integrated with micro

thermocouples and a Peltier chip, and a schematic control block diagram for fluid temperature controls. C Distinctive numbers ( $N_{spl}, N_{ref}$ ) of indicating channels that are filled with each fluid depending on the relative magnitude of the viscosity of the sample fluid ( $\mu_{spl}$ ) in relation to the reference fluid ( $\mu_{ref}$ ) at the same flow rate ( $Q_{spl} = Q_{ref}$ )

overcome the reduction in viscosity that occurs in a small channel, especially for blood due to a cell free layer (Barbee and Cokelet 1971; Fåhræus and Lindqvist 1931) and (c) the MCA composed of several indicating channels with identical channel dimensions. Figure 1C illustrates how a number of indicating channels filled with each fluid depend on the viscosity of the sample fluid in relation to the reference fluid at the same flow rate ( $Q_{\text{spl}} = Q_{\text{ref}}$ ). The sample and the reference fluids were injected simultaneously through an inlet (A) and an inlet (B). If the viscosity of the sample fluid is equal to that of the reference fluid ( $\mu_{\text{spl}} = \mu_{\text{ref}}$ ), then the number of indicating channels that become filled with each fluid is the same under the equal flow rate of the two fluids ( $N_{\text{spl}} = N_{\text{ref}}$ ), as shown in Fig. 1C(a). Furthermore, if the viscosity of the sample fluid is greater than that of the reference fluid ( $\mu_{\text{spl}} > \mu_{\text{ref}}$ ), then the number of indicating channels filled with the sample fluid will exceed the number filled with the reference fluid ( $N_{\text{spl}} > N_{\text{ref}}$ ), as depicted in Fig. 1C(b). Finally, the opposite ( $\mu_{\text{spl}} < \mu_{\text{ref}}$ ) also occurs when the viscosity of the sample fluid is less than that of the reference fluid ( $N_{\text{spl}} < N_{\text{ref}}$ ), as described in Fig. 1C(c).

### 2.3 Analytical formula of relative viscosity

The formula for the relative viscosity of the sample fluid in relation to the reference fluid can be derived by considering the flow rates for each fluid, the equivalent fluidic resistance of a diverging channel, and that of several indicating channels filled with each fluid.

Figure 2A shows the parameters considered in the derivation of the formula for relative viscosity. The microfluidic device was designed to have two inlets, a straight channel ( $W_s = 200 \mu\text{m}$ ), a diverging channel ( $r_B = 2,100 \mu\text{m}$ ), and 89 indicating channels ( $W_i = 50 \mu\text{m}$ ,  $L = 5,000 \mu\text{m}$ ,  $S = 23 \mu\text{m}$ , and depth =  $60 \mu\text{m}$ ). As illustrated in Fig. 2B, a mathematical model of the diverging channel filled with reference fluid can be expressed using cylindrical coordinates ( $e_r$ ,  $e_\theta$ , and  $e_z$ ). The flow rate ( $Q$ ) may be derived from a velocity profile (see Electronic Supplementary Material-S1). Through the manipulation of the relationship between the flow rate and the pressure drop ( $\Delta P$ ), a formula for the fluidic resistance of the diverging channel filled with the reference fluid can be determined:

$$R_{\text{ref,d}} = \mu_{\text{ref}} \left( \frac{\alpha}{N_{\text{ref}} W_i + (N_{\text{ref}} - 1) S} \right) \quad (1)$$

where  $\alpha$  is defined as

$$\alpha = \frac{12r_B}{h^3} \ln \left( \frac{r_B}{r_A} \right) \quad (2)$$

The subscripts ‘ref’ and ‘d’ refer to the reference fluid and the diverging channel, respectively. Additionally,  $N_{\text{ref}}$

indicates the number of indicating channels that become filled with the reference fluid.

The MCA is composed of a number of identical indicating channels with rectangular shapes (width =  $w$ , depth =  $h$ , and length =  $L$ ). It follows that each indicating channel that fills with reference fluid has the same fluidic resistance. Taking into account the fact that several indicating channels are connected in parallel, the formula for the fluidic resistance of the indicating channels ( $N_{\text{ref}}$ ) that become filled with the reference fluid in the MCA can be derived as:

$$R_{\text{ref,i}} = \frac{\mu_{\text{ref}} \gamma}{N_{\text{ref}}} \quad (3)$$

where  $\gamma$  is defined as:

$$\gamma = \frac{12L}{W_i h^3} \left( 1 - \frac{192h}{\pi^5 W_i} \sum_{n=1,3,5,\dots}^{\infty} \frac{1}{n^5} \tan h \left( \frac{n\pi W_i}{2h} \right) \right)^{-1} \quad (4)$$

The same procedures can be applied to determine the fluidic resistance of the diverging channel and the indicating channels that become filled with the sample fluid. The fluidic resistance of the diverging channel that is partially filled with sample fluid is therefore found to be:

$$R_{\text{spl,d}} = \mu_{\text{spl}} \left( \frac{\alpha}{N_{\text{spl}} W_i + (N_{\text{spl}} - 1) S} \right) \quad (5)$$

Similarly, the fluidic resistance of the indicating channels is:

$$R_{\text{spl,i}} = \frac{\mu_{\text{spl}} \gamma}{N_{\text{spl}}} \quad (6)$$

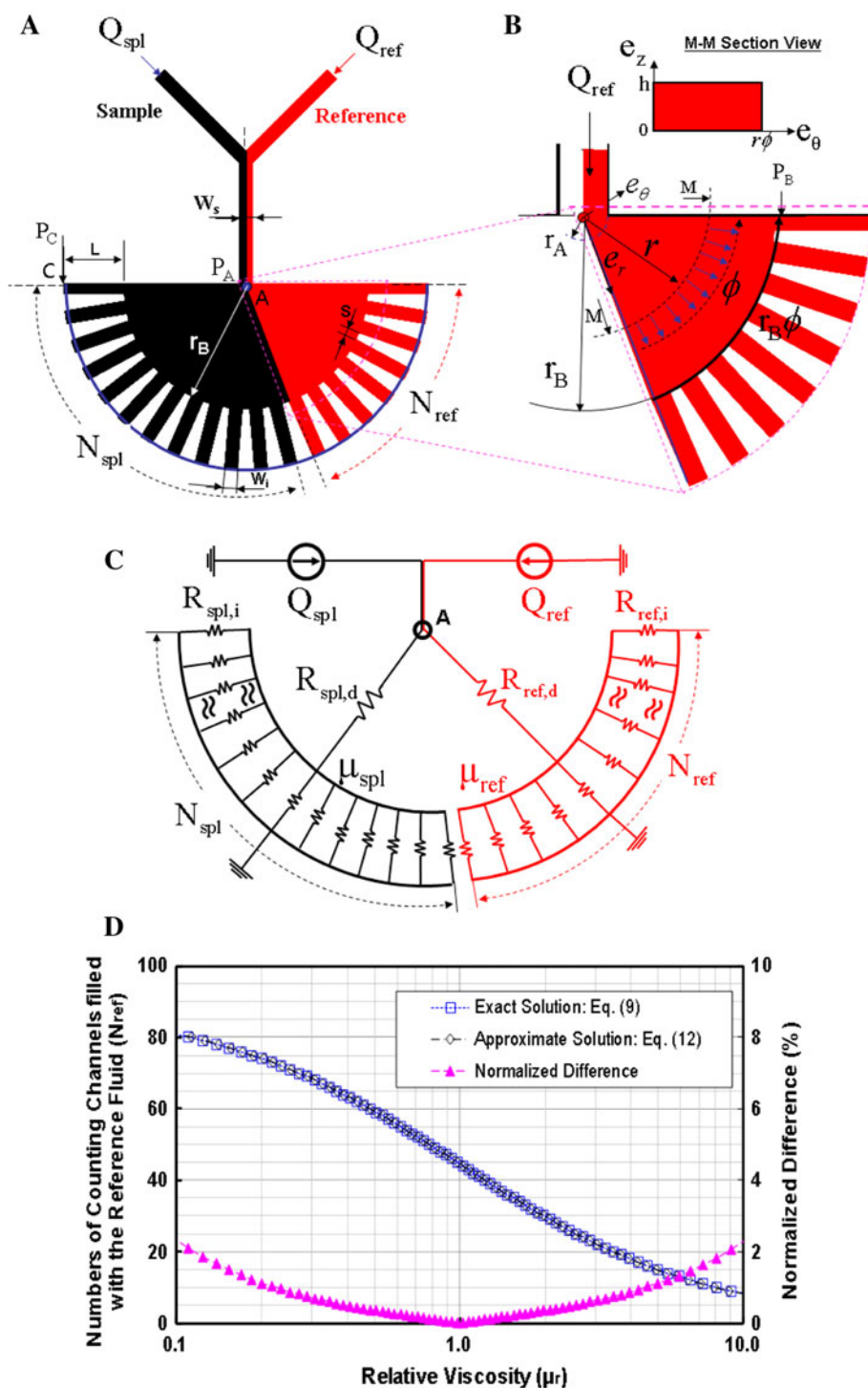
As shown in Fig. 2C, a lumped parameter model was developed that uses these analytical formulae for the fluidic resistance of the diverging channel and the indicating channels filled with each fluid. In addition, it is assumed that the compliance effect of the microfluidic channels is negligible. Given that the fluidic resistances of the diverging channel and of the indicating channels in the MCA are connected in series, the equivalent formulae for the fluidic resistance of the diverging and the indicating channels filled with the sample ( $R_{\text{spl,eq}}$ ) and the reference ( $R_{\text{ref,eq}}$ ) fluids can be written as:

$$R_{\text{spl,eq}} = \mu_{\text{spl}} \left[ \frac{\alpha N_{\text{spl}} + \gamma (N_{\text{spl}} W_i + (N_{\text{spl}} - 1) S)}{N_{\text{spl}} (N_{\text{spl}} W_i + (N_{\text{spl}} - 1) S)} \right] \quad (7)$$

$$R_{\text{ref,eq}} = \mu_{\text{ref}} \left[ \frac{\alpha N_{\text{ref}} + \gamma (N_{\text{ref}} W_i + (N_{\text{ref}} - 1) S)}{N_{\text{ref}} (N_{\text{ref}} W_i + (N_{\text{ref}} - 1) S)} \right] \quad (8)$$

By using the same pressure drop ( $\Delta P_{\text{spl}} = \Delta P_{\text{ref}}$ ) through a fluidic path that includes the diverging channel and the indicating channels that are filled with each fluid, the exact solution for the relative viscosity of the sample fluid in relation to the reference fluid then becomes:

**Fig. 2** An analytical study using a lumped parameter model for the proposed microfluidic viscometer. **A** Representative parameters for a straight channel ( $W_s = 200 \mu\text{m}$ ), a diverging channel ( $r_B = 2,100 \mu\text{m}$ ), identical indicating channels ( $W_i = 50 \mu\text{m}$ ,  $L = 5,000 \mu\text{m}$ ,  $S = 23 \mu\text{m}$ , and depth =  $60 \mu\text{m}$ ), injected flow rates for sample and reference fluids ( $Q_{spl}$ ,  $Q_{ref}$ ), and the number of indicating channels filled with the sample and reference fluids ( $N_{spl}$ ,  $N_{ref}$ ). **B** Major parameters used in the mathematical model of a diverging channel partially filled with the reference fluid. **C** A lumped parameter model of the proposed microfluidic device. Flow rates of the sample and reference fluids were modelled as  $Q_{spl}$  and  $Q_{ref}$ . In addition, friction losses in the microfluidic channels filled with sample and reference fluids were modelled as fluidic resistances ( $R_{spl}$ ,  $R_{ref}$ ). **D** A comparison between the exact solution and the approximate solutions for the indicating channels filled with reference fluid ( $N_{ref}$ ), compared with the relative viscosity of the sample fluid, and the normalized differences between the solutions



$$\mu_r = \left( \frac{\mu_{spl}}{\mu_{ref}} \right) = \delta_1 \delta_2 \left( \frac{N_{spl}}{N_{ref}} \right) \left( \frac{Q_{ref}}{Q_{spl}} \right)$$

where  $\delta_1$  and  $\delta_2$  may be written as

$$\delta_1 = \left[ \frac{\alpha N_{spl} + \gamma (N_{ref} W_i + (N_{ref} - 1) S)}{\alpha N_{spl} + \gamma (N_{spl} W_i + (N_{spl} - 1) S)} \right]$$

$$\delta_2 = \left[ \frac{N_{spl} W_i + (N_{spl} - 1) S}{N_{ref} W_i + (N_{ref} - 1) S} \right]$$

(10)

By considering the relative magnitude of the fluidic resistances of the diverging channel and the MCA with several identical indicating channels, it can be assumed that the order of magnitude of  $\alpha$  is much smaller than the order

of magnitude of  $\gamma$  in the coefficients  $\delta_1$  and  $\delta_2$ . In particular, it is reasonable to assume that  $\delta_1\delta_2 \approx 1$ . Therefore, an approximate solution for the relative viscosity of the sample fluid in relation to the reference fluid can be written as:

$$\mu_r = \left( \frac{\mu_{\text{spl}}}{\mu_{\text{ref}}} \right) \approx \left( \frac{N_{\text{spl}}}{N_{\text{ref}}} \right) \left( \frac{Q_{\text{ref}}}{Q_{\text{spl}}} \right) \quad (12)$$

According to Eq. (12), the viscosity of the sample fluid relative to the reference fluid can be determined by simply counting the number of microfluidic channels that become filled with the sample and reference fluids for the given flow rates. In Fig. 2D we compare the exact solution of Eq. (9) with the approximate solution of Eq. (12) for the number of indicating channels filled with the reference fluid ( $N_{\text{ref}}$ ) with respect to the relative viscosity of the sample fluid ( $\mu_r$ ). The results of this simulation show that the higher the viscosity ratio, the larger the normalized differences between the exact and approximate solutions. However, when the viscosity ratio is less than 10:1 ( $\mu_r = 0.1$ –10), the normalized differences between the two solutions is less than 2 %. Namely, the error caused by approximation is negligible. Thus, the results of this simulation imply that the approximate solution of Eq. (12) can be applied to determine the relative viscosity of the sample fluid with sufficient accuracy by ensuring that the MCA is designed with identical indicating channels, and that each channel has a much greater fluidic resistance than the diverging channel. In addition, the total number of indicating channels used clearly influences the accuracy of the result. An analysis of the errors in measurement, estimated theoretically, in relation to the total number of indicating channels shows that as expected, the use of a larger number of indicating channels tends to decrease the errors associated with measuring the viscosity. Therefore, it is important to select a suitable reference fluid, as well as the total number of indicating channels, for the proposed microfluidic viscometer (see Electronic Supplementary Material-S3 and S9).

#### 2.4 Formula for shear rate

Unlike Newtonian fluids, the viscosity of non-Newtonian fluids, such as blood depends on the shear rate. For this reason, the shear rate for each viscosity should be defined, especially in the measurement of the viscosity of blood. In the proposed microfluidic viscometer, the shear rate for each viscosity is defined at the indicating channel because the relative viscosity of the sample fluid relative to the reference fluid is determined in the MCA with identical indicating channels. In addition, we selected a Newtonian fluid to be the reference fluid, thereby ensuring that the viscosity was independent of the shear rate. For this reason, it is only necessary to define a shear rate for the sample fluid. In order

to estimate the shear rate of a sample fluid within a rectangular channel, and at a given flow rate of infusion, it is necessary to derive a formula that relates shear rate to flow rate. By using the flow rate and the shear stress formula for a rectangular duct (Truskey et al. 2004), the shear rate in an indicating channel filled with sample fluid is:

$$\dot{\gamma} = \left( \frac{6Q_{\text{spl}}}{W_i h^2 N_{\text{spl}}} \right) \left( \frac{\eta}{\xi} \right) \quad (13)$$

where  $\xi$  and  $\eta$  are represented as:

$$\xi = 1 - \frac{192h}{\pi^5 W_i} \sum_{n=1,3,5,\dots}^{\infty} \frac{1}{n^5} \tan h \left( \frac{n\pi W_i}{2h} \right) \quad (14)$$

$$\eta = 1 - \frac{16h}{\pi^3 W_i} \sum_{n=1,3,5,\dots}^{\infty} \frac{1}{n^3} \tan h \left( \frac{n\pi W_i}{2h} \right) \quad (15)$$

According to Eqs. (13), (14), and (15), the shear rate depends on several factors that include the delivery flow rate ( $Q_{\text{spl}}$ ) for the sample fluid, the number ( $N_{\text{spl}}$ ) of indicating channels filled with the sample fluid, and the width ( $W_i$ ) and depth ( $h$ ) of the indicating channels.

### 3 Experimental and methods

#### 3.1 Microfluidic viscometer and sample preparation

The proposed microfluidic viscometer consists of two parts. The first is a microfluidic device. For this, a PDMS (Polydimethylsiloxane) (Sylgard 184, Dow Corning, Korea) slab was first prepared using conventional PDMS replica moulding techniques (McDonald et al. 2000). In order to fabricate micro thermocouples for measuring the temperature of the fluids, copper and constantan were deposited equally on a glass substrate, via a microfabrication process, at a thickness of about 1  $\mu\text{m}$ , respectively (see Electronic Supplementary Material-S8). The PDMS slab and the glass substrate, which was integrated with micro thermocouples, were then treated with an oxygen plasma (CUTE, Femto Science, Korea), and bonded together. This newly created microfluidic device was then bonded to a Peltier chip (TEC1-24105, XYKM, China) using hot melt adhesives (ALCOWAX, Nikka Seiko Co., Japan).

The second part of the viscometer is a temperature controller for the fluids in the microfluidic device. The temperature controller was composed of a SMPS (VSF50-12, Orient Electronics, Korea), a solid-state relay (PDDo-105 N, Union Elecrom, Korea), and a feedback controller (CNi8DH24-C24, Omega Engineering, USA). Each component of the fluid temperature controller was connected to the microfluidic device according to the schematic diagram shown in Fig. S1 (see Electronic Supplementary Material-S2). The Labview program (National Instrument, USA) was used to

transfer the set temperatures to the fluid temperature controller via a RS-232C serial communication port.

Solutions of SDS that is a Newtonian fluid and blood that is a non-Newtonian fluid were applied as test fluids in order to verify the performance of our proposed microfluidic viscometer. In the case of the Newtonian fluid, five different concentrations (1.2, 3.2, 6.3, 11.9, and 20.3 %) of SDS diluted with DI water were prepared. In order to observe the indicating channels that were filled with each fluid, a solution of 0.03 % (v/v) polymer microspheres with red fluorescence (dia. 0.3  $\mu\text{m}$ , 1 % solids, Duke Scientific Corp.) was prepared in DI water and used as a reference fluid.

In the case of the non-Newtonian fluids (four different blood samples), the reference fluid was a solution of Phosphate Buffered Saline (PBS) (pH 7.4, Gibco, Invitrogen, USA). The hematocrit of the blood, which was donated by a blood bank (Chonam Blood Bank, Korea) was adjusted to 45 % using autologous plasma. Furthermore, in order to investigate the effect of the reduction of viscosity in the proposed microfluidic viscometer, rather than the dependence on shear rate, the blood sample was chemically fixed with glutaraldehyde (Abkarian et al. 2006; Baskurt et al. 2007) (see Electronic Supplementary Material-S5).

### 3.2 Experimental setup

After the preparation of the microfluidic viscometer and the test fluids (sample and reference fluids), the microfluidic device was mounted on an epi-fluorescence microscope (Olympus, Shinjuku, Japan) equipped with a cooled CCD camera DP-72 (Olympus, Japan). For the measurement of the viscosity of the SDS solution (Newtonian fluid), the reference and the sample (SDS solution) fluids were infused with a commercially available syringe pump (NEMESYS, Centoni GmbH, Germany). For the duration of the experiments, the temperature of both fluids was carefully maintained at 30 °C using the temperature controller. On the other hand, for the measurement of the viscosity of the blood (non-Newtonian fluid), the reference fluid and blood sample fluid were injected using the syringe pump. The temperature of both fluids was precisely maintained at 36 °C using the fluid temperature controller. After co-infusing the reference and sample fluids, snapshots of the number of the indicating channels filled with each fluid were captured by the cooled CCD camera. The number of indicating channels that were occupied by the reference fluid (or sample fluid) was then counted digitally. In order to evaluate the performance of the proposed microfluidic device quantitatively, the relative viscosity measured by the proposed microfluidic viscometer was compared with that measured by a commercially available viscometer (HAAKE MARS, Thermo Electron GmbH, Germany) equipped with a fluid temperature controller.

## 4 Results and discussion

### 4.1 Viscosity measurement for pure fluid (SDS)

#### 4.1.1 Experimental verifications

Solutions of SDS (Newtonian fluid) were applied to assess the accuracy of measurement of fluid viscosity identified by the proposed microfluidic viscometer. In order to demonstrate five different viscosities, five different concentrations of SDS solution was prepared. The proposed microfluidic viscometer was applied to measure fluid viscosity of the SDS solution. Then, the measurements obtained using these solutions were compared with those obtained by the conventional viscometer.

As shown in Fig. 3A, under five different concentrations of SDS solution [(a)  $C_{\text{SDS}} = 1.2\%$ , (b)  $C_{\text{SDS}} = 3.2\%$ , (c)  $C_{\text{SDS}} = 6.3\%$ , (d)  $C_{\text{SDS}} = 11.9\%$ , and (e)  $C_{\text{SDS}} = 20.3\%$ ], the microflow patterns that were captured by the epi-fluorescent microscope show the number of indicating channels that were filled with each fluid using the same flow rate for each (i.e.,  $Q_{\text{SDS}} = Q_{\text{ref}} = 1\text{ mL/h}$ ). The corresponding number of indicating channels that became filled with SDS solution were (a)  $N_{\text{sds}} = 46\text{--}47$  ( $N_{\text{ref}} = 42\text{--}43$ ), (b)  $N_{\text{sds}} = 50\text{--}51$  ( $N_{\text{ref}} = 38\text{--}39$ ), (c)  $N_{\text{sds}} = 56\text{--}57$  ( $N_{\text{ref}} = 32\text{--}33$ ), (d)  $N_{\text{sds}} = 63\text{--}64$  ( $N_{\text{ref}} = 25\text{--}26$ ), and (e)  $N_{\text{sds}} = 72\text{--}73$  ( $N_{\text{ref}} = 16\text{--}17$ ), respectively. These results indicate that higher concentrations of SDS solution resulted in a larger number of indicating channels filling with SDS solution. We determined the relative viscosity of the SDS solution using Eq. (9) to be (a)  $\mu_r = 1.09 \pm 0.02$  ( $C_{\text{SDS}} = 1.2\%$ ), (b)  $\mu_r = 1.31 \pm 0.03$  ( $C_{\text{SDS}} = 3.2\%$ ), (c)  $\mu_r = 1.74 \pm 0.04$  ( $C_{\text{SDS}} = 6.3\%$ ), (d)  $\mu_r = 2.49 \pm 0.07$  ( $C_{\text{SDS}} = 11.9\%$ ), and (e)  $\mu_r = 4.40 \pm 0.16$  ( $C_{\text{SDS}} = 20.3\%$ ). The conventional viscometer was used to verify the accuracy of each of these results, with measurements at each concentration obtained in triplicate ( $n = 3$ ). The relative viscosities of the SDS solutions were identified using the conventional method to be (a)  $\mu_r = 1.06 \pm 0.04$  ( $C_{\text{SDS}} = 1.2\%$ ), (b)  $\mu_r = 1.36 \pm 0.03$  ( $C_{\text{SDS}} = 3.2\%$ ), (c)  $\mu_r = 1.67 \pm 0.04$  ( $C_{\text{SDS}} = 6.3\%$ ), (d)  $\mu_r = 2.51 \pm 0.03$  ( $C_{\text{SDS}} = 11.9\%$ ), and (e)  $\mu_r = 4.19 \pm 0.05$  ( $C_{\text{SDS}} = 20.3\%$ ). As depicted in Fig. 3B(a), the relative viscosities obtained using our proposed microfluidic device were therefore in good agreement with those obtained using the conventional viscometer. In addition, the normalized differences between the two methods of viscosity measurement was less than 5 %, as illustrated in Fig. 3B(b). In order to examine the consistency of the viscosity measurements obtained using our proposed microfluidic viscometer, we carried out a detailed investigation of the change in relative viscosity of a solution of SDS (20.3 %) at several shear rates (see Electronic Supplementary

Material-S4). The results show that our proposed microfluidic viscometer can provide consistent measurements of viscosity at both high, and extremely low, shear rates. We therefore conclude that the proposed microfluidic device may be used to measure the viscosity of a Newtonian fluid (SDS solution) to an accuracy and consistency comparable to a commercially available viscometer.

#### 4.1.2 Numerical simulations

In order to evaluate the analytical solution and experimental results, a numerical simulation was conducted, and the results were compared with the relative viscosity of the

SDS solution as measured by the conventional viscometer. A commercially available CFD package was used to obtain the results of the numerical simulation. Throughout these studies, the flow rate at both inlets was fixed at 1 mL/h and the temperature of the two fluids was fixed at 30 °C. In addition, the mutual diffusion between the two fluids was neglected because the Péclet number was estimated to be approximately 90, even at a flow rate of 30  $\mu\text{L/h}$ , which was a minimum flow rate used in this study. Figure 3C shows the number of indicating channels with respect to the relative viscosity of the SDS solutions [(a)  $\mu_r = 1.36$  ( $C_{\text{SDS}} = 3.2\%$ ), (b)  $\mu_r = 1.67$  ( $C_{\text{SDS}} = 6.3\%$ ), (c)  $\mu_r = 2.51$  ( $C_{\text{SDS}} = 11.9\%$ ), and (d)  $\mu_r = 4.19$  ( $C_{\text{SDS}} = 20.3\%$ )].

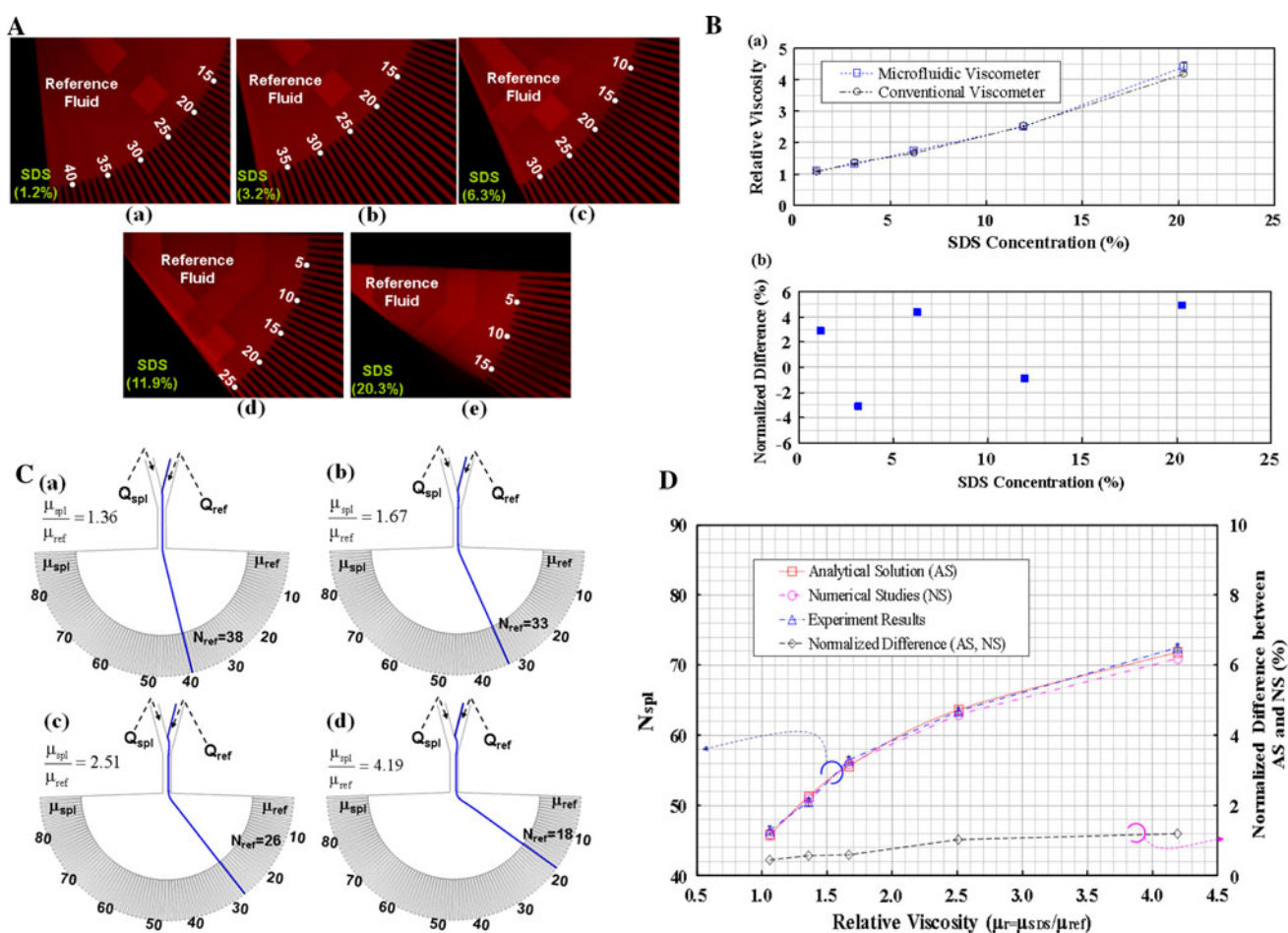


**Fig. 3** **A** Experimental results for the number of the indicating channels ( $N_{\text{ref}}$ ) filled with the reference fluid in a microfluidic channel array with respect to five different concentrations of SDS solution (a  $C_{\text{SDS}} = 1.2\%$ , b  $C_{\text{SDS}} = 3.2\%$ , c  $C_{\text{SDS}} = 6.3\%$ , d  $C_{\text{SDS}} = 11.9\%$ , and e  $C_{\text{SDS}} = 20.3\%$ ) for the same flow rate ( $Q_{\text{spl}} = Q_{\text{ref}} = 1\text{ mL/h}$ ). **B** A quantitative comparison of values for viscosity that were determined by both the proposed microfluidic viscometer and the conventional viscometer. a Relative viscosity and b normalized difference between the two methods against concentration of the SDS solution. **C** Results from numerical simulations of the number of

indicating channels filled with each fluid in the microfluidic channel array with respect to the relative viscosity of the sample fluid in relation to the reference fluid (a  $\mu_{\text{spl}}/\mu_{\text{ref}} = 1.36$ , b  $\mu_{\text{spl}}/\mu_{\text{ref}} = 1.67$ , c  $\mu_{\text{spl}}/\mu_{\text{ref}} = 2.51$ , and d  $\mu_{\text{spl}}/\mu_{\text{ref}} = 4.19$ ). **D** A comparison of the number ( $N_{\text{spl}}$ ) of indicating channels filled with the sample fluid, determined by three different methods: a analytical solution (AS), b numerical simulation (NS), c experimental results, and d the normalized difference between AS and NS with respect to relative viscosity



The numbers of indicating channels filled with the sample fluid were: (a)  $N_{\text{spl}} = 51$ , (b)  $N_{\text{spl}} = 56$ , (c)  $N_{\text{spl}} = 63$ , and (d)  $N_{\text{spl}} = 71$ .

#### 4.1.3 Comparison of three evaluation methods

Figure 3D shows the comparison of the number ( $N_{\text{spl}}$ ) of indicating channels that became filled with the sample fluid with respect to the relative viscosities ( $\mu_r$ ) obtained by analytical, numerical, and experimental methods. It can be seen that the results from the analytical solution are in good agreement with those obtained from the numerical simulation as well as with the experimental results. Furthermore, the normalized differences between the analytical and the numerical results were less than 2 %. These results therefore suggest that the analytical solution for relative viscosity may be used to determine the viscosity reasonably accurately, and may be applied simply by first counting the number of indicating channels that become filled with each fluid.

### 4.2 Viscosity measurement of complex fluid (blood)

#### 4.2.1 Normal blood in plasma and PBS suspensions

Normal blood typically behaves as a non-Newtonian fluid due to the effects of aggregation at low shear rates and the effect of deformability at high shear rates (Chien 1970). In order to evaluate the performance of the measurement of viscosity of a non-Newtonian fluid (normal blood), the proposed microfluidic viscometer was used to measure the viscosity of two different blood samples: (1) normal blood–plasma suspension (NBPL) and (2) normal blood–PBS suspension (NBPB).

The results for the viscosity of the NBPL are shown in Fig. 4A. Microflow patterns captured by the microscope were applied to count the numbers of indicating channels that became filled with normal blood–plasma and PBS at the same flow rates under the following conditions: (a)  $Q_{\text{NBPL}}/Q_{\text{PBS}} = 0.1/0.1$  mL/h, (b)  $Q_{\text{NBPL}}/Q_{\text{PBS}} = 0.3/0.3$  mL/h, (c)  $Q_{\text{NBPL}}/Q_{\text{PBS}} = 0.5/0.5$  mL/h, (d)  $Q_{\text{NBPL}}/Q_{\text{PBS}} = 1/1$  mL/h, (e)  $Q_{\text{NBPL}}/Q_{\text{PBS}} = 2/2$  mL/h, and (f)  $Q_{\text{NBPL}}/Q_{\text{PBS}} = 4/4$  mL/h. The corresponding number ( $N_{\text{NBPL}}$ ) of indicating channels that became filled with normal blood–plasma suspension were: (a)  $N_{\text{NBPL}} = 81$ –82, (b)  $N_{\text{NBPL}} = 76$ –78, (c)  $N_{\text{NBPL}} = 74$ –75, (d)  $N_{\text{NBPL}} = 72$ –73, (e)  $N_{\text{NBPL}} = 70$ –71, and (f)  $N_{\text{NBPL}} = 70$ –71. Using the formulas for relative viscosity (Eq. (9)) and shear rate (Eq. (13)), we found the relative viscosities ( $\mu_r = \mu_{\text{NBPL}}/\mu_{\text{PBS}}$ ) of the blood–plasma suspension in relation to PBS to be: (a)  $\mu_r = 11.64 \pm 0.36$  ( $\dot{\gamma} = 15.4 \text{ s}^{-1}$ ), (b)  $\mu_r = 6.47 \pm 0.39$  ( $\dot{\gamma} = 49.2 \text{ s}^{-1}$ ), (c)  $\mu_r = 5.03 \pm 0.25$

( $\dot{\gamma} = 85.2 \text{ s}^{-1}$ ), (d)  $\mu_r = 4.54 \pm 0.30$  ( $\dot{\gamma} = 174.2 \text{ s}^{-1}$ ), (e)  $\mu_r = 3.86 \pm 0.13$  ( $\dot{\gamma} = 357.8 \text{ s}^{-1}$ ), and (f)  $\mu_r = 3.74 \pm 0.11$  ( $\dot{\gamma} = 720.4 \text{ s}^{-1}$ ).

The results for the viscosity of the NBPB are illustrated in Fig. 4B. The captured microflow patterns were used to count the number of indicating channels filled with normal-PBS suspension and PBS at the following flow rates: (a)  $Q_{\text{NBPB}}/Q_{\text{PBS}} = 0.1/0.1$  mL/h, (b)  $Q_{\text{NBPB}}/Q_{\text{PBS}} = 0.2/0.2$  mL/h, (c)  $Q_{\text{NBPB}}/Q_{\text{PBS}} = 0.4/0.4$  mL/h, (d)  $Q_{\text{NBPB}}/Q_{\text{PBS}} = 0.5/0.5$  mL/h, (e)  $Q_{\text{NBPB}}/Q_{\text{PBS}} = 1/1$  mL/h, and (f)  $Q_{\text{NBPB}}/Q_{\text{PBS}} = 4/4$  mL/h. The corresponding numbers ( $N_{\text{NBPB}}$ ) of indicating channels filled with blood–PBS suspension were: (a)  $N_{\text{NBPB}} = 72$ –73, (b)  $N_{\text{NBPB}} = 71$ –72, (c)  $N_{\text{NBPB}} = 70$ –71, (d)  $N_{\text{NBPB}} = 68$ –69, (e)  $N_{\text{NBPB}} = 67$ –68, and (f)  $N_{\text{NBPB}} = 65$ –66. The relative viscosities ( $\mu_r = \mu_{\text{rNBPB}}/\mu_{\text{rPBS}}$ ) of blood–PBS suspension in relation to PBS were then determined to be: (a)  $\mu_r = 4.30 \pm 0.13$  ( $\dot{\gamma} = 17.5 \text{ s}^{-1}$ ), (b)  $\mu_r = 4.20 \pm 0.10$  ( $\dot{\gamma} = 35.2 \text{ s}^{-1}$ ), (c)  $\mu_r = 3.65 \pm 0.14$  ( $\dot{\gamma} = 72.4 \text{ s}^{-1}$ ), (d)  $\mu_r = 3.37 \pm 0.11$  ( $\dot{\gamma} = 92.1 \text{ s}^{-1}$ ), (e)  $\mu_r = 3.11 \pm 0.10$  ( $\dot{\gamma} = 187.5 \text{ s}^{-1}$ ), and (f)  $\mu_r = 2.70 \pm 0.10$  ( $\dot{\gamma} = 779.0 \text{ s}^{-1}$ ).

The conventional viscometer was also used in order to verify the accuracy of the values of blood viscosity determined using the proposed method. The viscosity of each blood sample was determined in triplicate ( $n = 3$ ). Figure 4C shows the comparison of the relative viscosities measured by the proposed microfluidic viscometer and the conventional viscometer for two different blood samples (NBPL, NBPB), with respect to various shear rates. The symbols (■, ●) indicate the relative viscosities measured by the conventional viscometer and the microfluidic viscometer for the normal blood–plasma suspension (NBPL).

In addition, the symbols (□, ○) represent the relative viscosities acquired by the conventional viscometer and the microfluidic viscometer for the normal blood–PBS suspension (NBPB). It can be seen that both the blood samples (NBPL, NBPB) behaved as non-Newtonian fluids, as expected. At low shear rates, the viscosity of the blood samples with normal blood–plasma was found to be higher than those with normal blood–PBS suspension due to the effects of aggregation. This illustrates the fact that normal blood–PBS suspension does not include proteins such as fibrinogen and immunoglobulins that induce aggregation effects (Chien 1970). Furthermore, the deformability of the two blood samples leads to a reduction in the relative viscosity at the higher shear rates. The different base solutions (plasma, PBS) at higher shear rates ( $\dot{\gamma} > 500 \text{ s}^{-1}$ ), also produce differences in viscosity.

In order to obtain a quantitative comparison of the accuracy of the relative viscosity measurements obtained from the two viscometers, the constant of proportionality ( $k$ ) and the exponent ( $n$ ) in the power law model

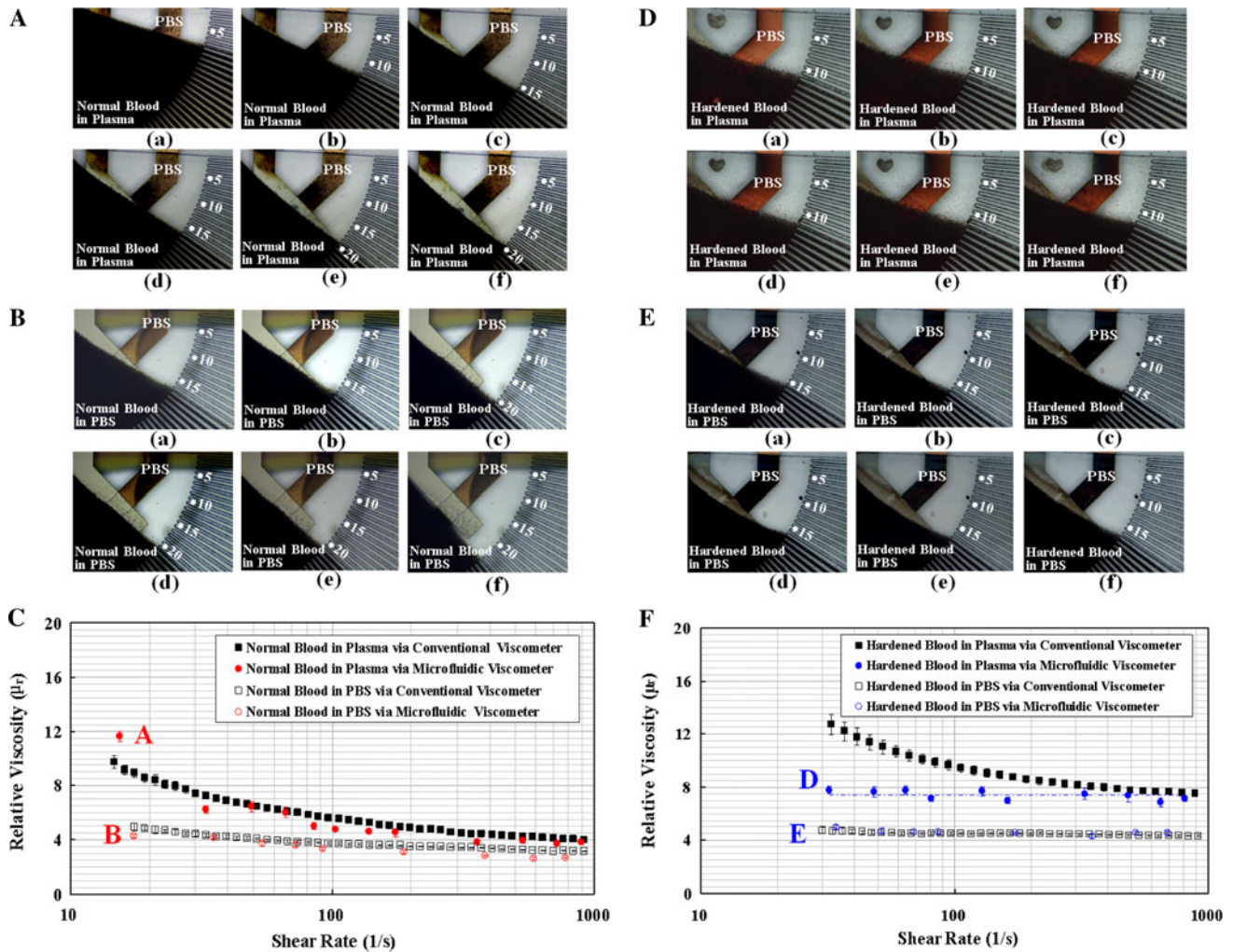


**Fig. 4** **A** Microflow patterns showing the number of indicating channels filled with normal blood–plasma suspension (NBPL) in relation to PBS with respect to various flow rates: *a*  $Q_{\text{NBPL}}/Q_{\text{PBS}} = 0.1/0.1$  mL/h, *b*  $Q_{\text{NBPL}}/Q_{\text{PBS}} = 0.3/0.3$  mL/h, *c*  $Q_{\text{NBPL}}/Q_{\text{PBS}} = 0.8/0.8$  mL/h, *d*  $Q_{\text{NBPL}}/Q_{\text{PBS}} = 1/1$  mL/h, *e*  $Q_{\text{NBPL}}/Q_{\text{PBS}} = 2/2$  mL/h, and *f*  $Q_{\text{NBPL}}/Q_{\text{PBS}} = 4/4$  mL/h. **B** Microflow patterns showing the number of indicating channels filled with normal blood–PBS suspension (NBPB) in relation to PBS with respect to various flow rates: *a*  $Q_{\text{NBPB}}/Q_{\text{PBS}} = 0.1/0.1$  mL/h, *b*  $Q_{\text{NBPB}}/Q_{\text{PBS}} = 0.2/0.2$  mL/h, *c*  $Q_{\text{NBPB}}/Q_{\text{PBS}} = 0.4/0.4$  mL/h, *d*  $Q_{\text{NBPB}}/Q_{\text{PBS}} = 0.5/0.5$  mL/h, *e*  $Q_{\text{NBPB}}/Q_{\text{PBS}} = 1/1$  mL/h, and *f*  $Q_{\text{NBPB}}/Q_{\text{PBS}} = 4/4$  mL/h. **C** A comparison of relative viscosity measured by the conventional viscometer and the proposed microfluidic viscometer for normal blood–plasma and normal blood–PBS suspension with respect to shear rate. **D** Microflow patterns showing the number of indicating

channels filled with hardened blood–plasma suspension (HBPL) in relation to PBS with respect to various flow rates: *a*  $Q_{\text{HBPL}}/Q_{\text{PBS}} = 0.2/0.2$  mL/h, *b*  $Q_{\text{HBPL}}/Q_{\text{PBS}} = 0.4/0.4$  mL/h, *c*  $Q_{\text{HBPL}}/Q_{\text{PBS}} = 0.8/0.8$  mL/h, *d*  $Q_{\text{HBPL}}/Q_{\text{PBS}} = 1/1$  mL/h, *e*  $Q_{\text{HBPL}}/Q_{\text{PBS}} = 2/2$  mL/h, and *f*  $Q_{\text{HBPL}}/Q_{\text{PBS}} = 4/4$  mL/h. **E** Microflow patterns showing the number of indicating channels filled with hardened blood–PBS suspension (HBPB) in relation to PBS with respect to various flow rates: *a*  $Q_{\text{HBPB}}/Q_{\text{PBS}} = 0.1/0.1$  mL/h, *b*  $Q_{\text{HBPB}}/Q_{\text{PBS}} = 0.2/0.2$  mL/h, *c*  $Q_{\text{HBPB}}/Q_{\text{PBS}} = 0.5/0.5$  mL/h, *d*  $Q_{\text{HBPB}}/Q_{\text{PBS}} = 0.5/0.5$  mL/h, *e*  $Q_{\text{HBPB}}/Q_{\text{PBS}} = 1/1$  mL/h, and *f*  $Q_{\text{HBPB}}/Q_{\text{PBS}} = 4/4$  mL/h. **F** A comparison of the relative viscosities measured by the conventional viscometer and the proposed microfluidic viscometer using hardened blood–plasma suspension and hardened blood–PBS suspension in relation to PBS

(Baskurt et al. 2007)  $\mu_r = k\dot{\gamma}^{n-1}$ ) were determined using the Least Squares Method (LSM). Firstly, for normal blood–plasma suspension, the  $k$  values for the microfluidic viscometer and the conventional viscometer were found to be 14.652 and 15.017, respectively, and the  $n$  values were found to be 0.771 and 0.795, respectively. The normalized differences in the two parameters ( $k$ ,  $n$ ) for the relative viscosity measured by the two viscometers were found to

be less than 3%. Secondly, for the normal blood–PBS suspension, the  $k$  values for the microfluidic viscometer and the conventional viscometer were found to be 6.49 and 6.269, respectively, and the  $n$  values were found to be 0.863 and 0.895, respectively. The normalized differences in the two parameters ( $k$ ,  $n$ ) for relative viscosity measured by the two viscometers were found to be less than 4%. These results indicate that our proposed microfluidic viscometer

can measure viscosity accurately for normal blood samples that behave as non-Newtonian fluids, compared with the results from a conventional viscometer.

#### 4.2.2 Hardened blood in plasma and PBS suspensions

Blood that has been chemically hardened with glutaraldehyde (0.8 %) normally behaves as a Newtonian fluid irrespective of the base solution, such as plasma and PBS, because the hardened blood is not influenced by deformability and aggregation. We analysed two different blood samples (hardened blood–plasma suspension and hardened blood–PBS suspension) in order to investigate the accuracy of our proposed technique for measuring viscosity. Figure 4D shows the number of indicating channels that became filled with hardened blood–plasma suspension (HBPL) and PBS at the same flow rates: (a)  $Q_{\text{HBPL}}/Q_{\text{PBS}} = 0.2/0.2$  mL/h, (b)  $Q_{\text{HBPL}}/Q_{\text{PBS}} = 0.4/0.4$  mL/h, (c)  $Q_{\text{HBPL}}/Q_{\text{PBS}} = 0.8/0.8$  mL/h, (d)  $Q_{\text{HBPL}}/Q_{\text{PBS}} = 1/1$  mL/h, (e)  $Q_{\text{HBPL}}/Q_{\text{PBS}} = 2/2$  mL/h, and (f)  $Q_{\text{HBPL}}/Q_{\text{PBS}} = 4/4$  mL/h. The corresponding number of indicating channels that became filled with the hardened blood–plasma suspension were: (a)  $N_{\text{HBPL}} = 78\text{--}79$ , (b)  $N_{\text{HBPL}} = 78\text{--}79$ , (c)  $N_{\text{HBPL}} = 78\text{--}79$ , (d)  $N_{\text{HBPL}} = 77\text{--}78$ , (e)  $N_{\text{HBPL}} = 78\text{--}79$ , and (f)  $N_{\text{HBPL}} = 77\text{--}78$ . As expected, these results show that the hardened blood–plasma suspension behaves as a Newtonian fluid because the number of indicating channels filled with hardened blood–plasma suspension was approximately the same ( $N_{\text{HBPL}} = 77\text{--}79$ ) for each of the six different flow rates. By using the formulas for relative viscosity and shear rate, we determined the relative viscosity ( $\mu_r = \mu_{\text{HBPL}}/\mu_{\text{PBS}}$ ) of hardened blood–plasma suspension ( $\mu_{\text{HBPL}}$ ) relative to PBS ( $\mu_{\text{PBS}}$ ), at each shear rate to be: (a)  $\mu_r = 7.78 \pm 0.30$  ( $\dot{\gamma} = 32.1 \text{ s}^{-1}$ ), (b)  $\mu_r = 7.74 \pm 0.33$  ( $\dot{\gamma} = 64.2 \text{ s}^{-1}$ ), (c)  $\mu_r = 7.71 \pm 0.35$  ( $\dot{\gamma} = 128.4 \text{ s}^{-1}$ ), (d)  $\mu_r = 7.01 \pm 0.24$  ( $\dot{\gamma} = 162.4 \text{ s}^{-1}$ ), (e)  $\mu_r = 7.50 \pm 0.42$  ( $\dot{\gamma} = 326.3 \text{ s}^{-1}$ ), and (f)  $\mu_r = 6.85 \pm 0.34$  ( $\dot{\gamma} = 651.3 \text{ s}^{-1}$ ). In addition, the hardened blood–PBS suspension (HBPB) was used to evaluate the accuracy of the viscosity measurements obtained using our proposed technique. As shown in Fig. 4E, microflow patterns were captured to measure the number of indicating channels that became filled with each fluid at the same flow rate: (a)  $Q_{\text{HBPB}}/Q_{\text{PBS}} = 0.2/0.2$  mL/h (b)  $Q_{\text{HBPB}}/Q_{\text{PBS}} = 0.4/0.4$  mL/h, (c)  $Q_{\text{HBPB}}/Q_{\text{PBS}} = 0.5/0.5$  mL/h, (d)  $Q_{\text{HBPB}}/Q_{\text{PBS}} = 1/1$  mL/h, (e)  $Q_{\text{HBPB}}/Q_{\text{PBS}} = 2/2$  mL/h, and (f)  $Q_{\text{HBPB}}/Q_{\text{PBS}} = 4/4$  mL/h. The corresponding number of indicating channels that became filled with the hardened blood–PBS suspension were: (a)  $N_{\text{HBPB}} = 74 - 75$ , (b)  $N_{\text{HBPB}} = 73 - 74$ , (c)  $N_{\text{HBPB}} = 73 - 74$ , (d)  $N_{\text{HBPB}} = 72 - 73$ , (e)  $N_{\text{HBPB}} = 72 - 73$ , and (f)  $N_{\text{HBPB}} = 73 - 74$ . Based on these results, the relative viscosities ( $\mu_r = \mu_{\text{HBPB}}/\mu_{\text{PBS}}$ ) of the hardened blood–PBS suspensions ( $\mu_{\text{HBPB}}$ )

relative to PBS ( $\mu_{\text{PBS}}$ ) were: (a)  $\mu_r = 4.98 \pm 0.14$  ( $\dot{\gamma} = 34.1 \text{ s}^{-1}$ ), (b)  $\mu_r = 4.64 \pm 0.16$  ( $\dot{\gamma} = 69.1 \text{ s}^{-1}$ ), (c)  $\mu_r = 4.66 \pm 0.17$  ( $\dot{\gamma} = 86.3 \text{ s}^{-1}$ ), (d)  $\mu_r = 4.54 \pm 0.08$  ( $\dot{\gamma} = 173.2 \text{ s}^{-1}$ ), (e)  $\mu_r = 4.29 \pm 0.13$  ( $\dot{\gamma} = 350.4 \text{ s}^{-1}$ ), and (f)  $\mu_r = 4.60 \pm 0.12$  ( $\dot{\gamma} = 691.8 \text{ s}^{-1}$ ). As expected, the hardened blood–PBS suspension was therefore also found to behave as a Newtonian fluid because the viscosity was not influenced by the shear rate.

In order to verify the performance of the viscosity measurements for two blood samples (hardened blood–plasma suspension, hardened blood–PBS suspension) with the proposed technique, the viscosity of each blood sample was also measured in triplicate using the conventional viscometer. Figure 4F shows the comparison of relative viscosity determined by the proposed microfluidic viscometer and the conventional viscometer for the hardened blood–plasma suspension and the hardened blood–PBS suspension with respect to various shear rates. Firstly, it can be seen that the hardened blood–PBS suspension behaves as a Newtonian fluid, as expected. The relative viscosities determined by the proposed microfluidic viscometer and the conventional viscometer were found to be  $4.63 \pm 0.19$ , and  $4.49 \pm 0.11$ , respectively, and the normalized difference between the two methods was less than 3 %. Secondly, according to the results from the proposed microfluidic viscometer, the hardened blood–plasma suspension was identified to be a Newtonian fluid, with a relative viscosity of  $7.39 \pm 0.33$ . However, the relative viscosity of this sample measured by the conventional viscometer showed non-Newtonian behavior, because the relative viscosity was found to depend on shear rate. We hypothesize that this unexpected result might have been due to the influence of aggregation rather than deformability. For this reason, the effect of aggregation was evaluated quantitatively by measuring the aggregation index (AI) (see Electronic Supplementary Material-S6). Analysis of these results leads us to the conclusion that the hardened blood cells–plasma suspension does indeed behave as a Newtonian fluid, and does not show any effects of aggregation. The non-Newtonian behavior determined by the conventional viscometer could be attributed to a surfactant layer formed by plasma proteins at the fluid–air interface of the cone and plate viscometer (Baskurt et al. 2007; Sharma et al. 2011). At higher shear rates ( $\dot{\gamma} > 600 \text{ s}^{-1}$ ), the relative viscosities were found to converge to  $7.58 \pm 0.08$ . In contrast, the proposed microfluidic viscometer does not include additional pressure drops due to a fluid–air interface in the microfluidic channel. The normalized difference between the proposed microfluidic viscometer and the conventional viscometer was less than 3 %. Lastly, in order to investigate blood viscosity reduction issues for the proposed microfluidic viscometer, the experimental results using the hardened blood–PBS suspension (HBPB) imply

that large spacious diverging channel with indicating channels can get over viscosity reduction problems (see Electronic Supplementary Material-S7).

It may therefore be concluded that our proposed microfluidic viscometer is capable of accurately measuring the viscosity of hardened blood samples, which behave as Newtonian fluids, notably without the calibration procedures, even artifacts when using a conventional viscometer.

## 5 Conclusion

In the study described herein, we successfully demonstrated an integrated microfluidic viscometer equipped with a fluid temperature controller. Using such a device, the viscosity of a fluid can be precisely and easily determined by counting the number of indicating channels that become filled with each of two fluids (sample and reference), especially when they are injected at the same flow rate. The fluid temperature controller, which uses a Peltier chip, micro thermocouples, and a feedback controller, was comprehensively investigated for maintain consistent fluid temperatures within the microfluidic channels. For accurate fluid viscosity identifications, an effective design criterion was discussed using an enhanced mathematical model for complex fluid networks. The accuracy of the proposed model was sufficiently investigated via numerical simulations as well as experimental measurements. As performance demonstrations, in the case of the Newtonian fluid (SDS), the proposed viscometer was able to measure viscosity accurately and consistently, and the normalized difference between the results obtained from this method and from a conventional viscometer was less than 5 %. Additionally, in the case of non-Newtonian fluids (blood), the proposed microfluidic viscometer was able to measure accurately the viscosity of two normal blood samples (non-Newtonian behaviour) and two hardened blood samples (Newtonian behaviour) without the need for any of the calibration procedures or artifacts confronted with a conventional viscometer. Future studies will apply this proposed microfluidic viscometer to the characterization of the rheological properties of blood for patients with various cardiovascular diseases. Furthermore, the measurement range demonstrated in this study might be considered as small (1 decade in viscosity) for wide applications. Thus, it will be required to enhance measurement ranges via unique methodologies including appropriate reference fluid selection, and flow rate ratio control (fixed numbers of indicating channel filled with each fluid).

**Acknowledgments** This study was partially funded by grants from the Ministry of Education, Science and Technology (MEST, KRF-20110028861), the Ministry of Education, Science and Technology

(NRF, No. 2010-0012897) and the Institute of Medical System Engineering (*iMSE*), GIST, Republic of Korea.

## References

- Abkarian M, Faivre M, Stone HA (2006) High-speed microfluidic differential manometer for cellular-scale hydrodynamics. *PNAS* 103:538–542
- Barbee JH, Cokelet GR (1971) The Fahraeus effect. *Microvasc Res* 3:6–16
- Baskurt OK, Hardeman MR, Rampling MW, Meiselman HJ (2007) *Handbook of Hemorheology and Hemodynamics*. 1st edn. IOS, pp 139–161
- Chevalier J, Ayela F (2008) Microfluidic on chip viscometers. *Rev Sci Instrum* 79:076102
- Chien S (1970) Shear dependence of effective cell volume as a determinant of blood viscosity. *Science* 168:977–979
- Fåhræus R, Lindqvist T (1931) The viscosity of the blood in narrow capillary tubes. *Am J Physiol Heart Circ Physiol* 96:562–568
- Guillot P, Panizza P, Salmon J-B, Joanicot M, Colin A (2006) Viscosimeter on a microfluidic chip. *Langmuir* 22:6438–6445
- Guillot P, Moulin T, Kotitz R, Guirardel M, Dodge A, Joanicot M, Colin A, Bruneau C-H, Colin T (2008) Towards a continuous microfluidic rheometer. *Microfluid Nanofluid* 5:619–630
- Han Z, Tang X, Zheng B (2007) A PDMS viscometer for microliter Newtonian fluid. *J Micromech Microeng* 17:1828–1834
- Kang K, Lee LJ, Koelling KW (2005) High shear microfluidics and its application in rheological measurement. *Exp Fluids* 38:222–232
- Kang YJ, Yoon SY, Lee K-H, Yang S (2010) A highly accurate and consistent microfluidic viscometer for continuous blood viscosity measurement. *Artif Organs* 34:944–949
- Keen S, Yao A, Leach J, Leonardo RD, Saunter C, Love G, Cooper J, Padgett M (2009) Multipoint viscosity measurements in microfluidic channels using optical tweezers. *Lab Chip* 9:2059–2062
- Lan WJ, Li SW, Xu JH, Luo GS (2010) Rapid measurement of fluid viscosity using co-flowing in a co-axial microfluidic device. *Microfluid Nanofluid* 8:687–693
- Lee J, Tripathi A (2005) Intrinsic viscosity of polymers and biopolymers measured by microchip. *Anal Chem* 77:7137–7147
- Lin Y-Y, Lin C-W, Yang L-J, Wang A-B (2007) Micro-viscometer based on electrowetting on dielectric. *Electrochim Acta* 52:2876–2883
- McDonald JC, Duffy DC, Anderson JR, Chiu DT, Wu H, Schueller OJA, Whitesides GM (2000) Fabrication of microfluidic systems in poly (dimethylsiloxane). *Electrophoresis* 21:27–40
- Nguyen N-T, Yap Y-F, Sumargo A (2008) Microfluidic rheometer based on hydrodynamic focusing. *Meas Sci Technol* 19:085405
- Pipe CJ, Majmudar TS, McKinley GH (2008) High shear rate viscometry. *Rheol Acta* 47:621–642
- Quist A, Chand A, Ramachandran S, Cohen D, Lal R (2006) Piezoresistive cantilever based nanoflow and viscosity sensor for microchannels. *Lab Chip* 6:1450–1454
- Sharma V, Jaishankar A, Wang Y-C, McKinley GH (2011) Rheology of globular proteins: apparent yield stress, high shear rate viscosity and interfacial viscoelasticity of bovine serum albumin solutions. *Soft Matter* 7:5150–5160
- Srivastava N, Davenport RD, Burns MA (2005) Nanoliter viscometer for analyzing blood plasma and other liquid samples. *Anal Chem* 77:383–392
- Truskey GA, Yuan F, Katz DF (2004) *Transport phenomena in biological systems*. 1st edn. Pearson Prentice Hall, pp 139–161